Behaviour of Piezoelectric Ceramics under Various Environmental and Operation Conditions of Radiating Sonar Transducers

by

D. A. Berlincourt and H. H. A. Krueger

Electronic Research Division, Clevite Corporation, Cleveland 8, Ohio

ABSTRACT

Design of transducers for lower frequency high power density, and deeper submersion puts increasing demands on piezoelectric transducer materials. It has been demonstrated that appropriate lead titanate zirconate ceramics can operate under high bias stress and at high power levels without failure. However, changes in physical properties, especially in permittivity as a result of a change in static compressive stress and changes in permittivity and tan∂ with drive amplitude, have become increasingly of concern.

The mechanisms whereby the nonlinear characteristics of ferroelectric ceramics bring about: dependence of physicalproperties on electric and mechanical stress are discussed. The basic differences in behaviour under high electric and mechanical stress of alkaline earth-substituted lead titanate zirconate ("hard") and -doped lead titanate zirconate ("soft") are outlined. Data are given also for a new "Very hard" lead titanate zirconate, PZT-8. Stabilizing treatments which tend to minimize pressure effects are described.

Emphasis on behaviour under environmental and operating conditions is placed on the following:

1) Variations in the piezoelectric constant d_{33} and permittivity with static compressive stress parallel to the polar axis.

2) Changes of permittivity with time under maintained stress.

3) Changes of permittivity and tan∂ with electric field at various levels of compressive stress parallel to the polar axis.Variations in permittivity and d_{33} with stress cycling (stress parallel to the polar axis).

I. INTRODUCTION

To understand the behaviour of piezoelectric ceramics under various environmental and operation conditions it is necessary to develop an understanding of the origin of nonlinearities in these materials. The very existence of a piezoelectric effect in these ceramics depends upon a very nonlinear near process termed poling, and yet the term "piezoelectric" infers a linear relationship between an applied electric field or charge and a generated mechanical stress or strain or vice versa.

With a nonferroelectric piezoelectric crystal such as quartz or ammonium dihydrogen phosphate these relationships are strictly linear except for weak higher order effects which can occur in significant amounts only at input signals greater than the dielectric or mechanical strength. With ferroelectric ceramics nonlinearities result from domain effects [1]) and in fact the linear piezoelectric effect is generally enhanced by reversible domain wall motion.

In radiating sonar transducers nonlinearities of the piezoelectric ceramics result in amplitude dependent dielectric and mechanical. losses (heat power) and in distortion of the output acoustic signal. In general significant distortion occurs only at input electric fields well beyond those at which dielectric or mechanical losses become a limiting factor. This is related to the fact that the strain-electric field relationship remains reasonably linear to considerably higher electric fields than does the charge-electric field relationship. [2])

In this paper the behaviour of piezoelectric ceramics under various environmental and operating conditions will be discussed with special emphasis on nonlinear effects, since these not only directly affect the performance of transducers but also because their onset marks a sort of elastic or electric limit on the amplitude to which these materials may be driven.

II. ORIGIN OF NONLINEARITY

The polar axis of a perovskite ferroelectric may be oriented parallel to an edge (tetragonal), a body diagonal (rhombohedral), or a face diagonal, (orthorhombic) of the pseudocubic perovskite cell. The polar direction is elongated with respect to its length in the reference cubic phase. In each case 180° domain reorientation can take place. This will here be termed "electrical" domain reorientation, since this is the main type of orientation which occurs with high electric drive, and since reorientation of this type takes

place with no nonpiezoelectric mechanical strain. The other type of domain reorientation is termed "mechanical" since it involves dimensional changes. This is by 90° in a tetragonal perovskite, by 120°-60° or 90° in an orthorhombic perovskite. and by 109°-71° in a rhombohedral perovskite.

The distortion from the reference cubic phase in barium titanate in tetragonal in a range near room temperature, and Its value is about 1%. Lead titanate zirconates may have either tetragonal or rhombohedral distortion. and their values are about 2% and 0.7% respectively. Very roughly it may be stated that coercive electric fields are higher with larger distortion and that there is also a relationship to mechanical coercivity. The rhombohedral lead titanate zirconates generally have smaller linear ranges for instance, than do the tetragonal lead titanate zirconates. An important exception to this rule occurs with the donor type additives {Nb^{5+} for $(Ti,Zr)_{4+}$ or La_{3+} for Pb_{2+}} to lead titanate zircons. They do not have a major effect on the distortion but they severely reduce mechanical and electrical coereivity.[3]) The alkaline earth substitutions for lead also have relatively little effect on distortion, but they tend to Increase slightly mechanical and electrical coercivity.

Piezoelectric ceramics which will be discussed here are PZT-4, PZT-5A, barium titanate with calcium substitution for barium and barium titanate with calcium and cobalt or calcium and lead. PZT-4 is characteristic of the "hard" lead titanate zirconates with alkaline earth substition for lead and PZT-5A is characteristic of the "soft" lead titanate zirconates with donor type additives. Data will also be given for a newly developed "very hard" lead titanate zirconate, PZT-8.

III. **BEHAVIOUR AT HIGH ELECTRIC INPUT**

Figure 1 shows tan∂ as a function of electric field for several piezoelectric ceramics at 25°C. The increase in dielectric loss is due to nonlinearity In the dielectric displacement-electric field relationship (hysteresis) caused primarily by electrical (180°) domain reorientation. Figure 1 shows also the variation of the free permittivity (ε^T_{33})

with electric field for these same compositions at 25°C The increase of dielectric loss with increasing electric field lowers electromechanical or electroacoustic efficiency and generates heat. The change of permittivity with electric field upsets inductive tuning of the clamped capacitance In sonar transducers.

Figure 2 shows similar data at elevated temperatures for the same ceramic compositions. The superiority of the "hard" lead titanate zirconate compositions is even more pronounced here than at 25°C. These data are, of course, not identical for every specimen of a given composition. and for a given specimen the value of tan∂ at each level of electric field is lower the longer the elapsed time between poling and electric field exposure. Figure 3 shows permittivity and tan∂ vs electric field for PZT-4 specimens from a single batch, but poled at different times. The upper curve in each case is typical 24 hours after poling; this is generally the standard for comparison of various materials and 24-hour data were plotted in Fig. 1. It should be emphasized that a major disturbance such as exposure to a temperature of 150 to 200°C or a stress of 10,000 to 20,000 psi acts to de-age the ceramic. Permittivity and tan∂ vs electric field plots on aged specimens so exposed are more nearly like those for relatively freshly poled specimens. This is shown in Figs. 4 and 5 for PZT-4 and PZT-8 respectively. Note that the effects of exposure to 150°C for five minutes are considerably more severe than those of exposure to 10,000 psi parallel stress for ten minutes.

These data, however, do not in themselves constitute a criterion for high power applications, since the different materials have widely different piezoelectric constants and therefore provide different mechanical amplitude at a given electric field. One should instead compare materials on the basis of dielectrically dissipated heat power an function of acoustic power. The dielectrically dissipated heat power density (watts/m^3) is given by:

$$p_{DE} = \omega E^2_3 \varepsilon^T_{33} \tan\partial$$

where E is rms electric field in V/m. The acoustic power density (watts/m3) In a simple mass-loaded. transducer exclusive of any mechanical losses is given by:

$$p = \omega E^2_3 k^2 \varepsilon^T_{33} Q_M$$

where Q_M is the effective Q of the transducer.

Figures 6 and 7 show dielectrically dissipated beat power (calculatedusing the tan ∂-field curves of Figs. 1 and 2) as a function of acoustic power (watts/cm^3 kcps) with a transducer Q of three for several compositions.*

With p_{DE} limited to 0.2 watts/cm^3 kcps. acoustic powers are 1.3, 2.8, 4.1,10, and 17.5 for the five compositions at 25°C.

In general depolarization of ceramic compositions as a result of high dynamic electric fields occurs at amplitudes well beyond any used in sonar transducers. Figure 8 shows effects of exposure to high electric fields at 60 cps. Temperature was externally controlled so these effects are independent of dielectric heating. Depolarization results from the one half cycles in which the field is directed such that it causes 180° domain reversals. Effects of negative dc electric fields are much more drastic but since sonar transducers are not exposed to such operating conditions this will not be discussed further.

*For the parallel mode (k_{33}).

IV. BEHAVIOUR UNDER HIGH MECHANICAL STRESS

The effects of high mechanical stress are in general dependent upon the orientation of the stress with respect to the polar axis of the ceramic, the electrical load, and frequency. For sonar one is not concerned with electric response to large amplitude static or dynamic stress, although this is an important consideration in high voltage generating systems. This discussion will be limited to consideration of the effects of static or dynamic stress on the electroelastic constants of piezoelectric ceramics. Static stress is provided either by a mechanical biasing arrangement or deep submersion or generally by a combination of both. Dynamic stress is piezoelectrically generated and static mechanical bias is provided in order to eliminate or at least to reduce tensile stress.

A. Dynamic Stress

Figure 9 shows mechanical Q and Youngto Modulus (ls^E) of three ceramics as functions of dynamic stress. These measurements were made using the circumferential mode of a ring in order to have uniform stress and the measurements were carried to mechanical failure. [4]) Neglecting all mechanical losses other than in the ceramic, heat power due to mechanical losses in a simple mass-loaded transducer is given approximately by:

$$p_{DM} = \frac{pQ_M}{Q_C} = \omega_r E^2_3 \varepsilon^T_{33} k^2 Q_M{}^2 / Q_C$$

where Q_C is the mechanical Q of the ceramic. Figure 10 shows p_{DM} and P_{DE} for PZT-4 as functions of acoustic power for a loaded Q of three (dashed curves). With this value of loaded Q, heat power due to mechanical losses is roughly comparable to that due to dielectric losses. With higher loaded Q, p_{DM} becomes predominant and with lower values p_{DE} is predominant.

Data are not yet available on the variation of Q c with stress amplitude for PZT-8, but the low amplitude value is over 1000 with one week's aging, roughly twice that for PZT-4. Figure 10 also shows (p_{DE}+p_{DM}) as function of acoustic power with Q_M = 3 for PZT-4, PZT-8, and 95w% $BaTiO_3$, 5w% $CaTiO_3$. Values of P_{DM} for PZT-8 are estimated. Limiting the total dissipated power to 0.2 watts/cm kcps, values of acoustic power are respectively 11, 5, and 2.2 for PZT-8, PZT-4, and 95/5 BCT. Figure 11 is a plot of these same data to a linear scale, properly emphasizing differences in power handling capacities. All losses in the ceramic except those due to piezoelectric phase angles are included. Losses due to piezoelectric phase angles are probably also highest for materials with lowest electrical and mechanical Q. It is thought that power dissipated due to piezoelectric phase angles, p_{DME}, is somewhat less than P_{DE} or P_{DM} .

*The Q_c- stress characteristic for the parallel mode is assumed the same as that for the lateral mode (Fig.9).

B. Static Stress

In operation a deep submersion sonar transducer is subject to a constant static stress (bias) plus a slowly or periodically variable additional compressive stress provided by the sea water load. One is concerned then with changes in physical properties, especially permittivity and piezoelectric constant; with time under maintained stress and with changes due to variable stress. Effects are dependent on orientation of stress with respect to the polar axis.[5-10]) Effects are also much different for different compositions. In order to prevent unnecessary complexity in this discussion a brief review of the different types of behaviour will be made and then specific data will be given for PZT-4 and PZT-8 for parallel compression only.

There are in general two types of lead titanate zirconate compositions, as mentioned earlier, those with donor type substitutions ("soft") and those with alkaline earth substitutions ("hard"). As a general rule the latter are used in radiating transducers, the former in hydrophones. The "soft" materials generally suffer degradation with stress which is much more dependent upon the number of stress cycles than upon total period of stress exposure. They should generally therefore not be used with variable static stress. The "hard" materials are not subject to this limitation, but their properties are functions of the magnitude of the stress.

Compression parallel to the polar axis reduces the perfection of domain alignment by mechanical (other than 180°) reorientation, as it tends to force polar axes into the allowed position closest to the plane perpendicular to the compressive stress. Since the permittivity of perovskites parallel to the polar axis of a domain is less than that perpendicular to the polar axis, this causes an increase in the dielectric constant ε^T_{33} and a decrease ε^T_{11} The reorientation tends to reduce the piezoelectric effect since it reduces the volume of material contributing directly to this effect. This is countered by an increase in the number of domain walls and their contribution to the piezoelectric effect, so that the piezoelectric coupling factors are affected much less by stress than is the permittivity. The increase in the number of domain walls tends also to increase compliance and permittivity, and these domain wall contributions are lossy. Mechanical and electrical Q's both degrade.

Stress perpendicular to the polar axis also causes mechanical domain reorientation, tending to force polar axes into the allowed position closest to the plane perpendicular to the stress. Since most of the domains have their polar axes fairly close to this plane as a result of poling, there is less domain switching with lateral stress and changes in permittivity and compliance are less severe than with longitudinal compression. The piezoelectric constants are, however, severely affected by lateral compression, since

*Changes in Young's modulus are less important in low-Q radiating sonar transducers.

the domain reorientation itself subtracts from the loaded piezoelectric constant (d_{31} with bias stress T_1) and adds to the unloaded piezoelectric constant (d_{32} with bias stress T_1).

Two-dimensional compression in the plane perpendicular to the polar axis is effective in mechanically orienting polar axes of domains into the allowed direction most nearly parallel to the polar axis. This stress therefore acts only on domains not oriented during poling; it must be noted that the improved orientation by stress is nonpolar (random ±). This has a strong effect in decreasing permittivity, but should have little effect on piezoelectric coupling. Hydrostatic compression has relatively little effect on domain configuration; and therefore effects on piezoelectric and dielectric constants are less severe than with any other compressive stress configuration. [6])

In this discussion effects of parallel stress will be considered in detail, and methods to increase stability will be described. For a variety of reasons this mode of operation has become predominant in sonar transducers. with bias stress. mechanical displacement. and driving electric field all parallel to the polar axis.

Figure 12 shows permittivity as function of slowly varying parallel compressive stress for PZT-4. Permittivity first increases sharply and then decreases slightly with stress increase, and there is pronounced hysteresis with stress decrease. It is thought that this peculiar behaviour in associated with the fact that PZT-4 Is just on the tetragonal side of the rhombohedral-tetragonal phase boundary. For comparison data for a "PZT-4" with a few atom % more Ti^{4+} , and therefore safely tetragonal, are shown in Fig. 13. The anomaly found with PZT-4 is here absent. The data in Figs. 12 and 13 also show the de-aging effect of the stress (note increase In tan∂ as a result of the first stress cycle). The stabilizing effect of the first stress cycle is also shown.

A much wore effective means to stabilize a lead titanate zirconate ceramic for future stress cycles is to heat the material to about 200°C for an hour or so. The effect on the tan 8 and permittivity vs electric field characteristics (see Figs. 4 and 5) should, however. be kept in mind. Figure 14 shows permittivity as function of parallel stress for PZT-4 so stabilized. For comparison the characteristic is also shown for material only mechanically prestabilized (copy of the fourth cycle data of Fig. 12). The thermal prestabilizing treatment results in a decrease of about 10% in the coupling factor and an increase of 10% or more in permittivity, but it substantially reduces changes in permittivity and piezoelectric constant with stress.

Figure 15 shows the variation of d_{33} with parallel stress for PZT-4 with and without temperature prestabilization. For comparison the variation of d_{33} with parallel stress is shown also for unstabilized tetragonal "PZT-4". The effectiveness of the prestabilizing treatment is clearly shown.

Figures 16 and 17 show ε^T_{33} and d_{33} as functions of parallel stress for stabilized PZT-8. Behaviour is superior to that shown in Figures 14 and 15 for PZT-4.

One is, of course, concerned with the changes of parameters not only with changes in static stress, but also with time at a given static stress. As discussed briefly earlier, a change in static stress, a large change in temperature, or exposure to a high ac or dc electric field starts a new aging cycle. Strictly speaking the aging rate in this new cycle depends upon history, such as the length of time since poling, previous exposure to high stress, etc. Because of the logarithmic nature of the aging process, however, the influence of past events is somewhat obscured, particularly when the subsequent event is a major one.

Figure 18 shows permittivity as function of the log of time for PZT-4, the upper curve with 10,000 psi and the lower curve with 20,000 psi parallel stress maintained. Aging rates are respectively -1.3 and -2.6% per time decade. For comparison the. typical aging rate for freshly poled PZT-4 under ambient conditions is -5.8% per time decade. The aging data of Fig. 18 were obtained on specimens poled about one month earlier; under ambient conditions 100hours additional aging corresponds to only about 0.06 decade and a change of only about -0,35%. Total changes in the period 0.1 to 100 hours were -4.2% at 10,000 psi and -8,4% at 20 000 psi. The data of Fig. 18 do, however, show that continued exposure to high parallel stress does not create a runaway situation.

Figure 19 shows aging of the piezoelectric constant d 33 with maintained 10,000 psi parallel compression. There is an upward drift and then a leveling off; with greater exposure time d_{33} would begin to decrease. Figure 19 also shows aging of the lateral d-constants (d_{31}, d_{32} with maintained lateral stress (T_1). As mentioned previously, the stress acts to decrease the loaded constant (d_{31}) and increase the unloaded constant (d_{32}), but both age downward, the former very sharply.

V. **EFFECTS OF SIMUTANEOUS EXPOSURE TO HIGH STATIC STRESS AND HIGH ELECTRIC FIELD**.

So far this discussion has been limited to c consideration of effects individually of high electric field and high static or dynamic stress. In actual operation one encounters a combination of all three. Actually high ac electric field under nonresonant conditions creates dynamic strains not very far removed from those encountered in operation of sonar radiating devices with loaded Q generally less than five. A nonresonant electric field of 5 kV/cm rms, for Instance. creates an rms strain of about 1.5×10^{-4} in PZT-4.

Behaviour with combined high ac electric field and high static stress has been studied only quite recently. * one would be inclined to expect the tan∂ vs electric field characteristic to degrade under high static stress.

It has been shown that static stress exposure starts a new aging cycle, and also that the tan∂ vs electric field characteristic improves with time after a major disturbance. Figures 4 and 5 show the degradation in the characteristic resulting from previous stress or high temperature exposure.

Figure 20 shows tan∂ and permittivity as functions of ac electric field at various levels of parallel compressive stress for well aged (about one month) PZT-4. Degradation of the tan∂-electric field characteristic is immediately evident at 5,000 Psi and there is very little further deterioration up to 20,000 psi. Comparison of Figures 4 and 20 shows that the tan∂ vs field characteristic is about the same for an aged specimen immediately after a short exposure to 150°C or with maintained compressive stress in the 10,000 to 20,000 psi range. It is interesting to note that there is immediate partial recovery upon release of the compressive stress (Figs. 4 and 5). This immediate recovery does not occur upon cooling after a temperature cycle.

Figure 20 also shows the deterioration of the permittivity - electric field characteristic under stress. Total changes with stress are decreased by a prestabilizing treatment.

Figure 21 shows tan∂ and permittivity as functions of ac electric field for PZT-8 at various levels of parallel compressive stress.

Behaviour is similar to that shown for PZT-4, with tan∂ at each value of electric field approximately doubled by axial stress in the range 5,000 to 20,000 psi. The originally superior characteristics of PZT-8' are especially important in that these characteristics remain superior by about the same margin under static compression.

It should be noted that with strongly piezoelectric materials (those with piezoelectric coupling greater than about 0.50) there is a strong correlation between dielectric and mechanical losses. Under circumstances in which one is increased the other in general also increases; this is a natural result of strong electromechanical coupling. The deleterious effects on dielectric losses as a result of mechanical bias (Figs. 20 and 21) must be accompanied also by similar effects on mechanical losses. Thus the mechanical loss-stress characteristics (converse of Fig. 9) must worsen under mechanical bias. This characteristic must also degrade as a result of a disturbance which acts to de-age the ceramic. Such disturbances are, again, exposure to high electric field, mechanical stress, and/or a temperature cycle.

* -In this work combined effects of high electric field and parallel static stress are discussed. See reference 6) for a discussion of combined effects of hydrostatic pressure and high electric field.

SUMMARY

Some of the effects of high static and dynamic stress and electric field on the characteristics of piezoelectric ceramics have been described. It was demonstrated that with lead titanate zirconate ceramics changes in physical characteristics with these parameters are a more serious problem than depolarization or permanent degradation of the Piezoelectric effect. It was also shown that heat power losses due to the active element in radiating transducers are dependent upon past thermal, electrical; and mechanical history and bias mechanical stress as well as driving electric field and dynamic mechanical stress. Proper choice of piezoelectric ceramic and use of a simple stabilizing technique are effective means of reducing variation of physical characteristics with static stress and high electrical and mechanical drive.

FIGURE CAPTIONS

Fig. 1. Tan∂ and ε^T_{33} vs electric field for several piezoelectric ceramics at 25°C.

Fig. 2. Tan∂ and ε^T_{33} vs electric field for several piezoelectric ceramics. The data are for 100°C for the lead titanate zirconate ceramics, 80°C for the barium lead calcium titanate, and 75°C for the barium calcium titanate.

Fig. 3. Tan∂ and ε^T_{33} vs electric field for PZT-4 specimens from a single batch poled at different times. The uppermost curve of each set is typical 24 hours after poling; the lowest curve of each act is typical one or more months after poling.

Fig. 4. Tan∂ and ε^T_{33} vs electric field for PZT-4 The lowest curve of each set is for an aged (over one month) specimen. The upper curve of each set is for a fragment of the same specimen which was exposed to 150°C for five minutes just prior to this test. The other curve of each set is for a similar fragment exposed to 10,000 psi parallel stress for ten minutes just prior to this test.

Fig. 5. Same as Figure 4, but for PZT-8.

Fig. 6. Dielectrically dissipated heat power p_{DE} as function of acoustic power for several ceramic compositions. A simple mass-loaded transducer with loaded Q_M of three is assumed. The numbers beside each point give the driving electric field in kV/cm. Temperature 25°C,

Fig. 7. Same as Figure 6, but temperature is 100°C for the lead titanate zirconate composition and 75-80°C for the barium titanate compositions.

Fig. 8. Depolarization resulting from about 30 minutes' exposure to indicated values of 60 cps electric field and temperature for PZT-4 and barium titanate ceramic.

Fig. 9. Dependence of internal mechanical Q (Q_M) and Young's modulus $1/s^E_{11}$ on dynamic stress amplitude for PZT-4, PZT-5A, and 95 wt $BaTiO_3$ with 5 wt % $CaTiO_3$* Dynamic stress perpendicular to polar axis.

Fig, 10. Internal beat due to dielectric and mechanical losses ($p_{DE} + p_{DM}$) as function of acoustic power for several ceramic compositions. A simple mass-loaded transducer with loaded Q of three is assumed. The dashed lines show P_{DM} and P_{DE} separately as functions of acoustic power for PZT-4. Temperature 25°C.

Fig. 11. Same as Figure 10, but a full linear scale is used rather than log-log. This allows rapid comparison to scale of power handling capacities.

Fig. 12. ε^T_{33} and tan∂ vs slowly varying parallel compressive stress for PZT-4 (not stabilized). Data are shown for the first and fourth stress cycle.

Fig. 13. Same as Figure 12, but data are for a strongly tetragonal "PZT-4" (not stabilized).

Fig. 14. ε^T_{33} vs slowly varying parallel compressive stress to 20,000 psi for thermally stabilized and unstabilized PZT-4. Data are shown for the fourth stress cycle. A fifth cycle to 10,000 psi is also shown for stabilized PZT-4.

Fig 15. d_{33} vs slowly varying parallel compressive stress to 20,000 psi for thermally stabilized and unstabilized PZT-4, and unstabilIzed tetragonal "PZT-4." The three lower curves are each for the fourth stress cycle to 20,000 psi. The upper curve is for a cycle to 12,000 psi after four cycles to 20,000 psi.

Fig. 16. Permittivity vs parallel compressive stress to 20, 000 psi for thermally stabilized PZT-8. Data are shown for the fourth cycle to 20,000 psi and for a cycle to 10,000 psi after 50 cycles to 20,000 psi.

Fig. 17. d_{33} vs parallel compressive stress to 20,000 psi for thermally stabilized PZT-8. Data are shown for the fourth cycle to 20,000psi and for a cycle to 10.000 psi after 50 cycles to 20,000 psi.

Fig. 18. ε^T_{33} vs time for unstabilized PZT-4 with 10,000 and 20,000 psi parallel compressive stress. Stress maintained.

Fig. 19. Aging of d_{33} with 10.000 psi compressive stress (T_3) parallel to the polar axis and aging of d_{31} and d_{32} with 10,000 psi compressivestress (T_1) perpendicular to the polar axis for PZT-4. Stress maintained.

Fig. 20. Tan∂ and ε^T_{33} vs ac electric field at various levels of parallel compressive stress for well aged (about one month) PZT-4.

Fig. 21. Same as Figure 20. but for PZT-8.

REFERENCES

1. D. Berlincourt and H. H. A. Krueger, J. Appl. Phys. 30, 1804 (1959).
2. G. Schmidt, Z. Physik. 148, 314 (1957),
3. R. Gerson and Hans Jaffe,, J. Phys. Chem. Solids 24, 979 (1963).
4. R. Gerson,, J. Acoust. Soc. Am. 32. 1297 (196o).
5. D. Berlincourt and H. H. A. Krueger,, J. Acoust. Soc. Am. 33; 1339 (1961).
6. R. Y. Nishi and R. F. Brown, J. Acoust. Soc. Am. 36, 1292 (1964).
7. R. F. Brown, Can. J. PhyB. 392 741 (1961).
8. R. F. Brown and G. W. McMahon, Can. J. Phys. 40, 672 (1962).
9. I. A. Uhak and D. A. Shugurov, Soviet Phys.-Tech. PhYs. 3p 486 (1958).
10. S. V. Bogdanov, B. M. Vul, and R. Ya. Razbash. Soviet Phys.-Cryst. 6,

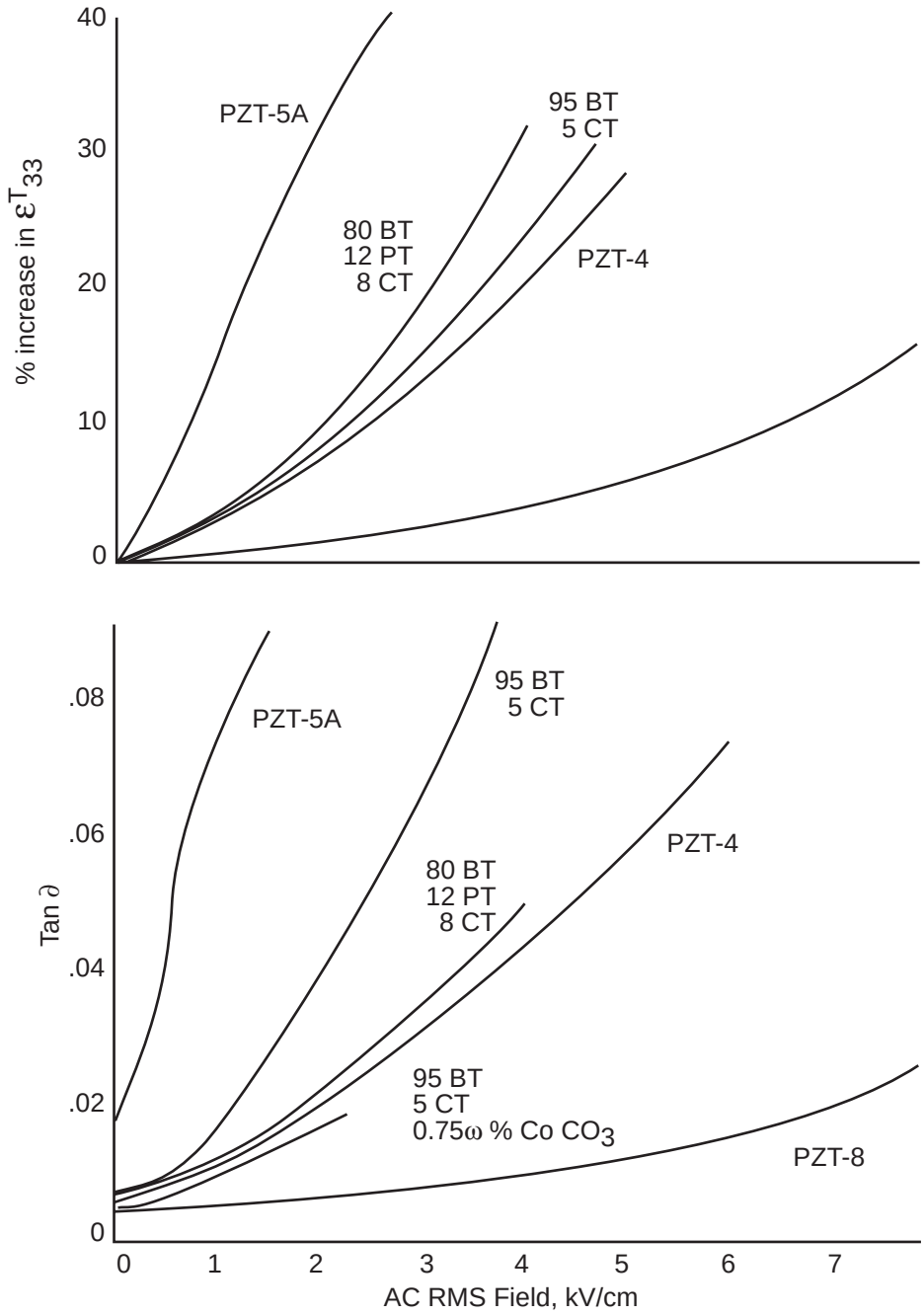

Fig. 1 ε^T_{33} and tan∂ vs Electric Field, 25*C4

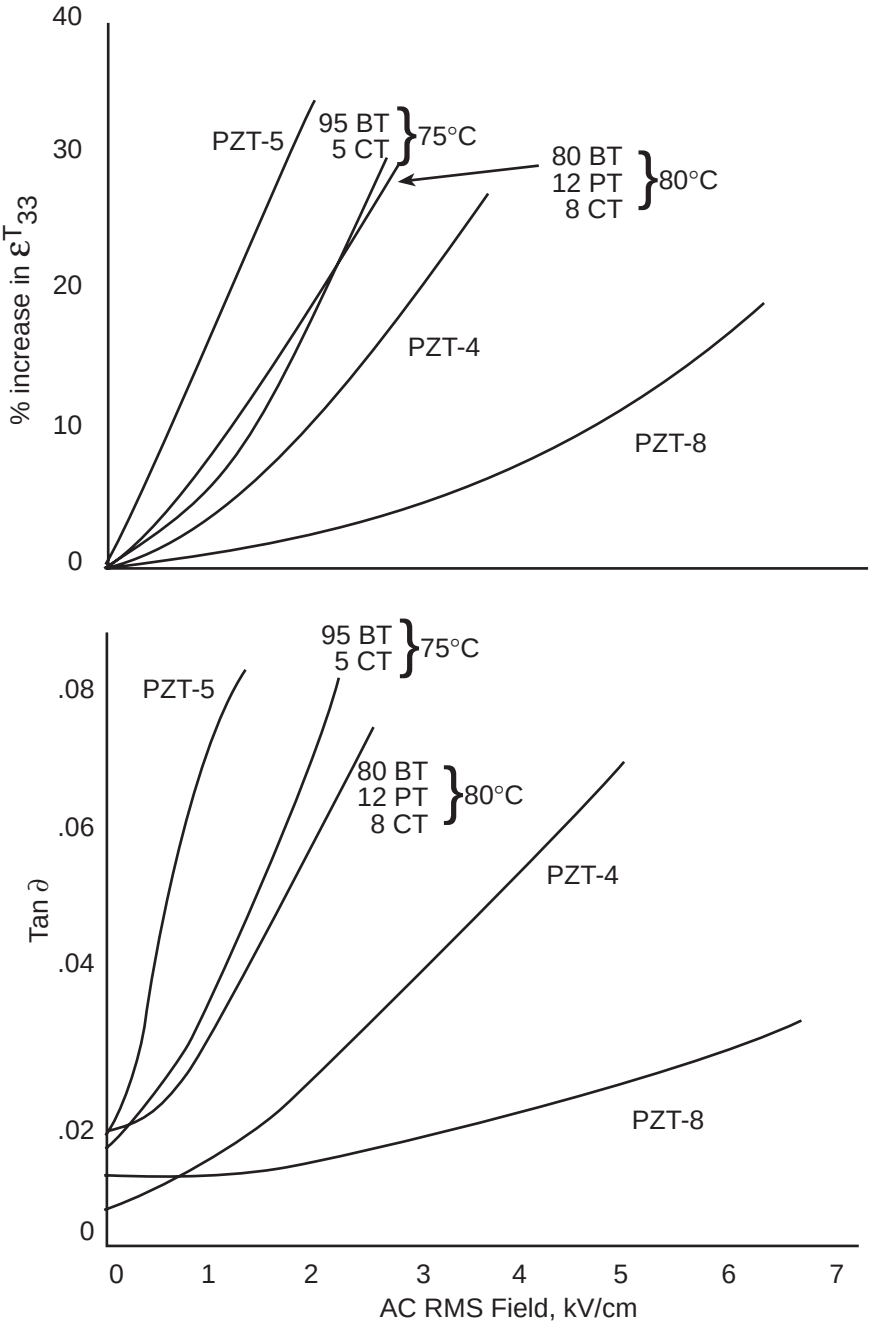

Fig. 2 $\varepsilon^T_{33} / \varepsilon_o$ and tan∂ vs Electric Field, 100*C4

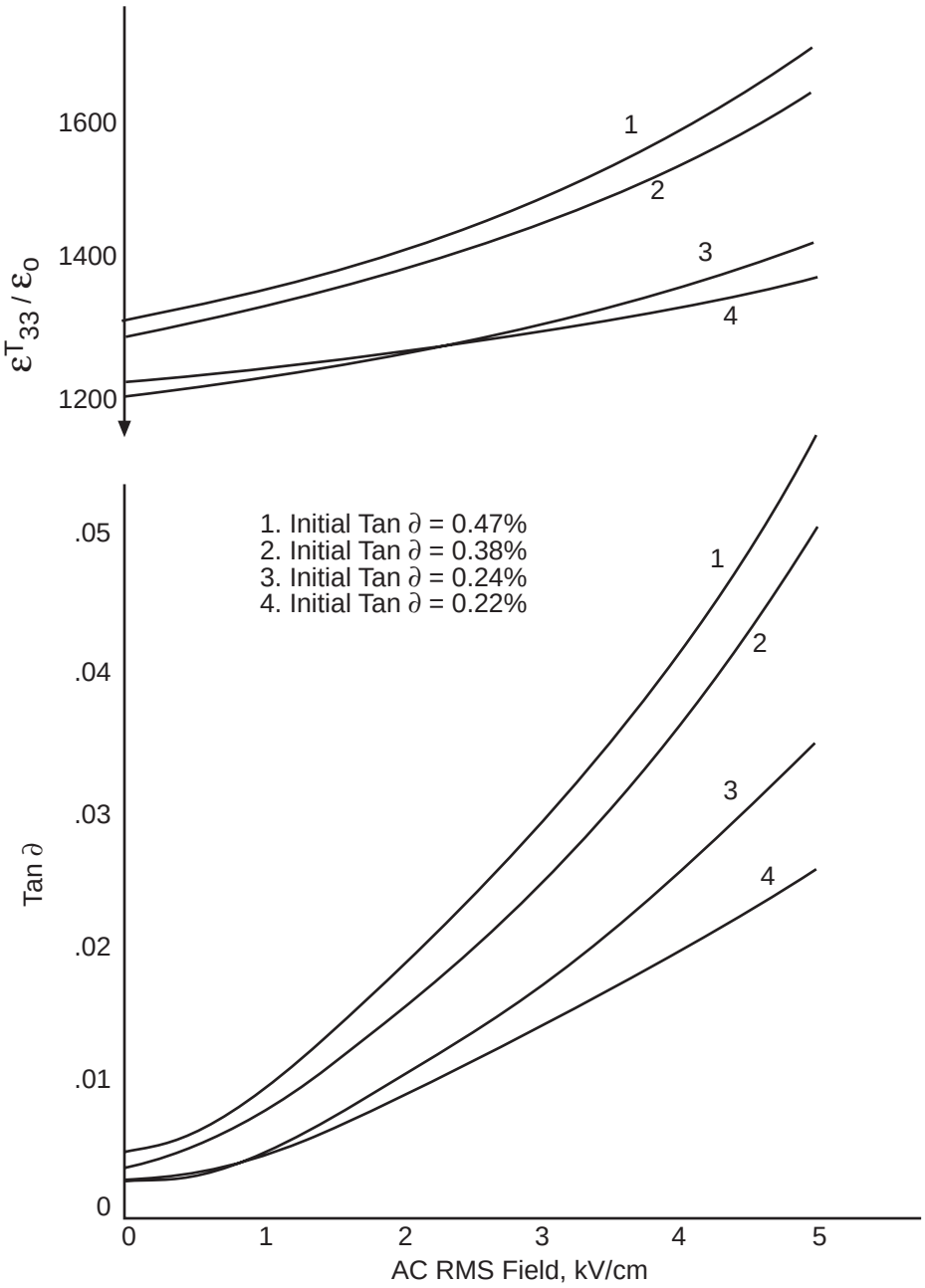

Fig. 3 $\varepsilon^T_{33} / \varepsilon_o$ and tan∂ vs Electric Field; Specimens of PZT-4

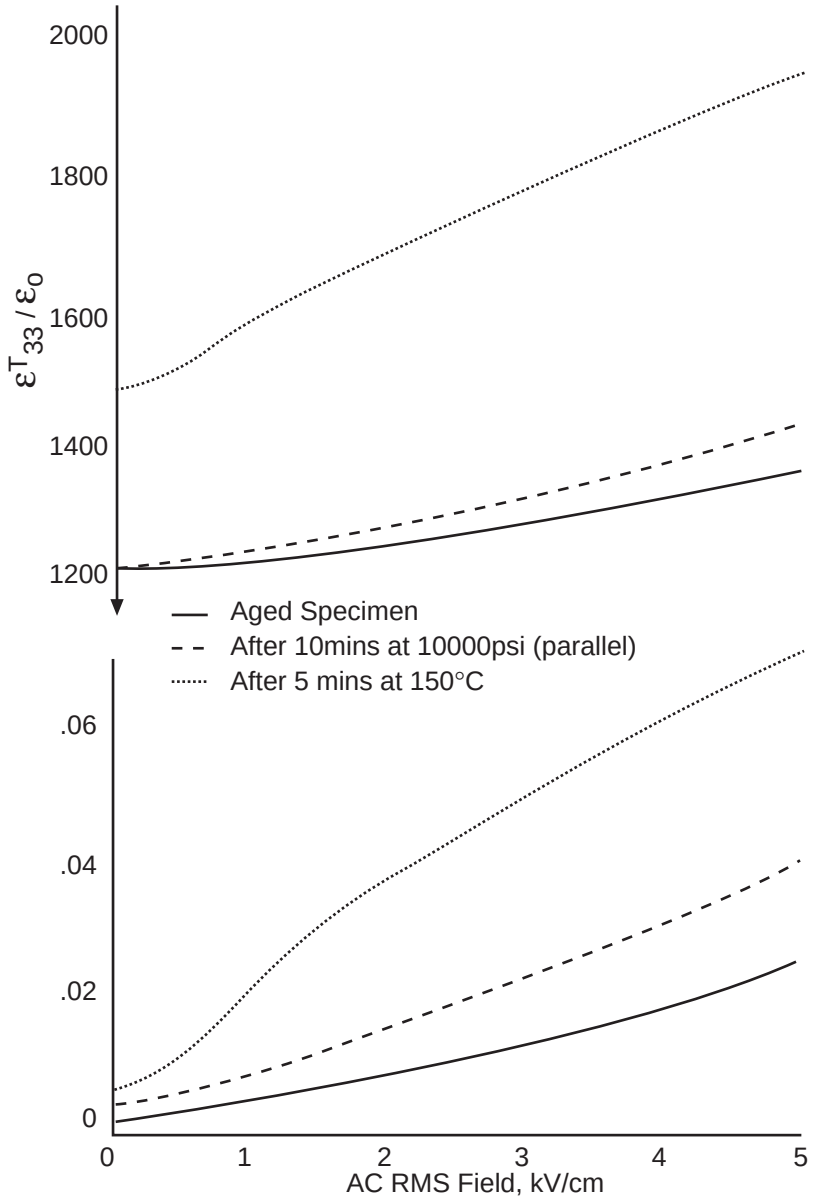

Fig. 4 $\varepsilon^T_{33} / \varepsilon_0$ and tan∂ vs Electric FieldPZT-4

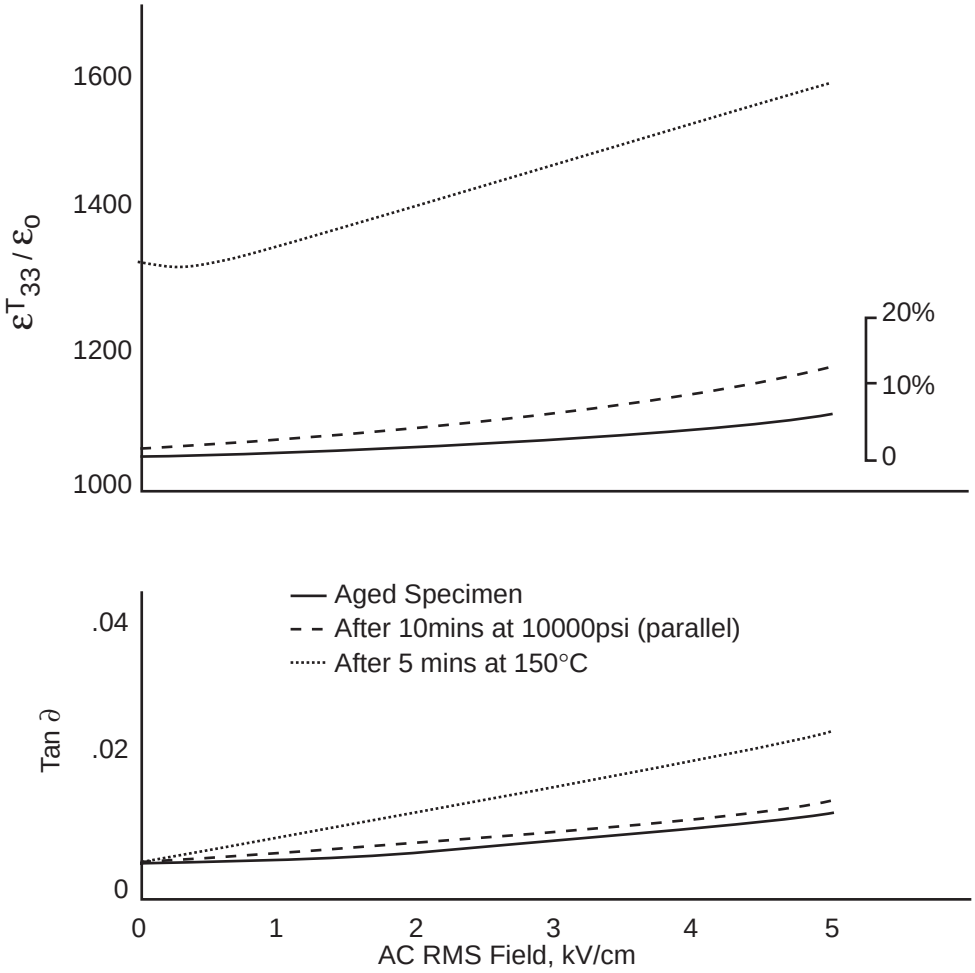

Fig. 5 $\varepsilon^T_{33} / \varepsilon_o$ and tan∂ vs Electric Field PZT-8

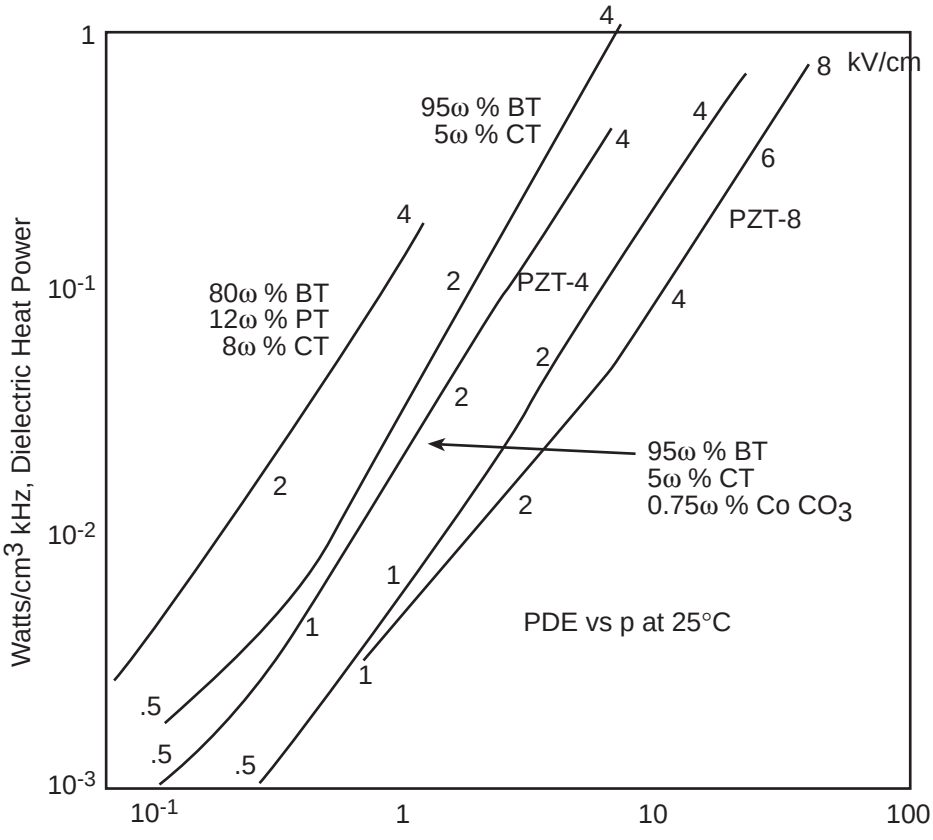

Fig. 6 Acoustic Power Q_M=3, in Watts/cm^3 kHz

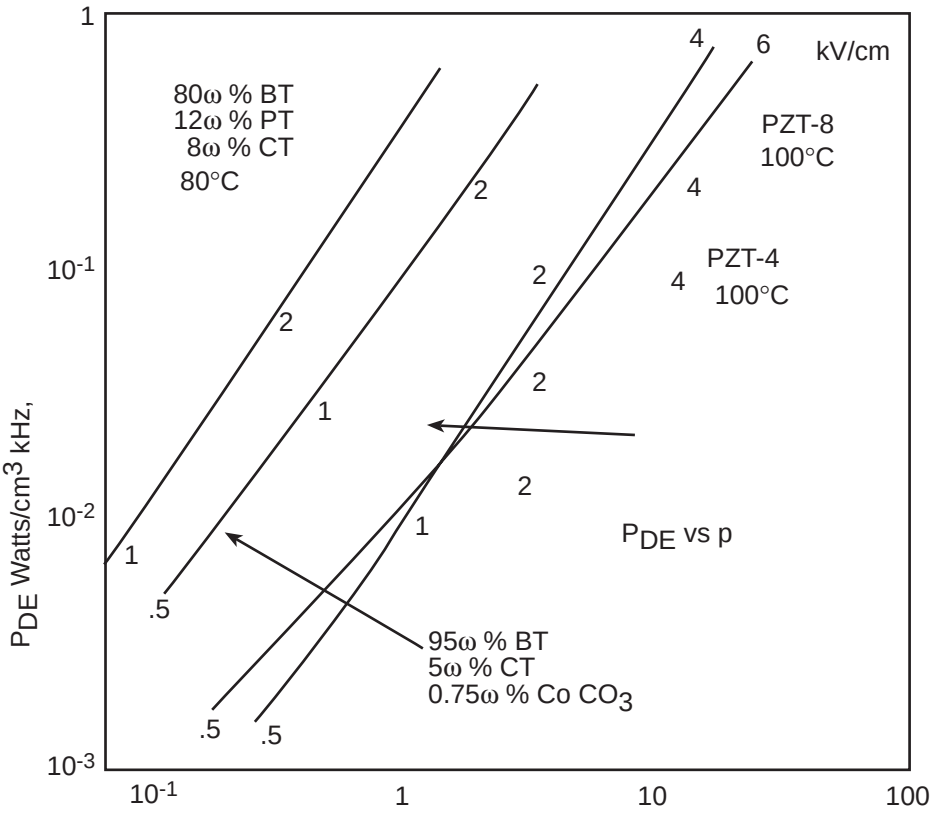

Fig. 7 P with Q_M=3, in Watts/cm^3 kHz

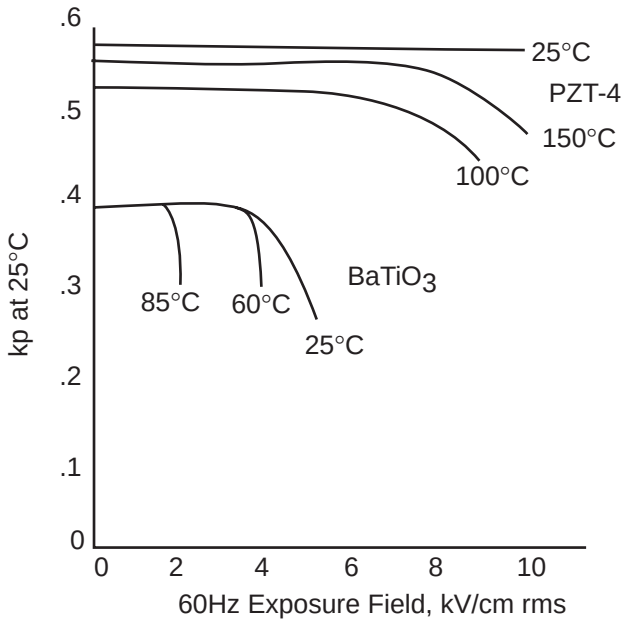

Fig. 8 Depolarization resulting from about 30 mins exposure to indicated values of 60Hz electric field and temperature for PZT-4 and $BaTiO_3$

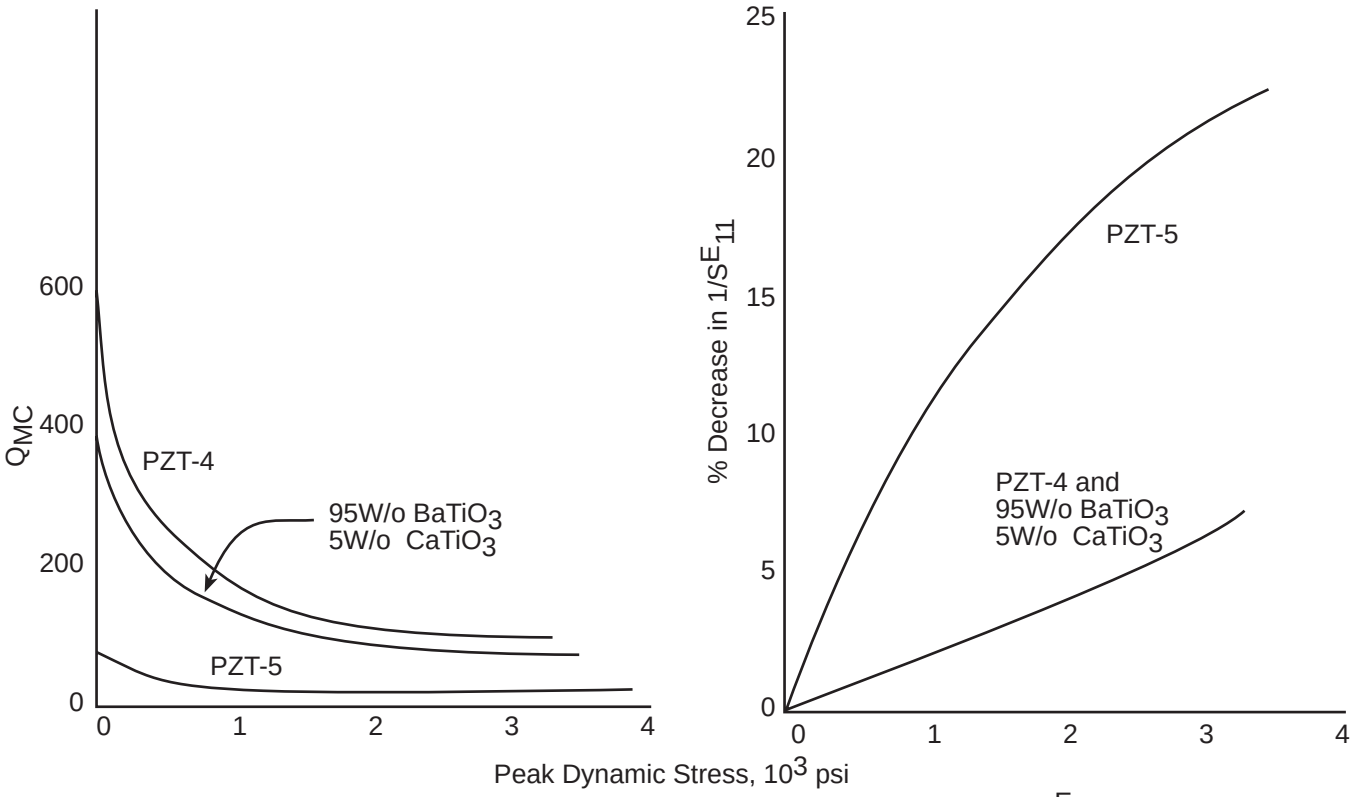

Fig. 9 Dependence on internal mechanical Q (Q_{MC}) and Young's Modulus ($1/S^E_1$) on dynamic stress amplitude for PZT-4, PZT-5, and 95W/o $BaTiO_3$ with 5W/o $CaTiO_3$. Dynamic stress perpendicular to polar axis.

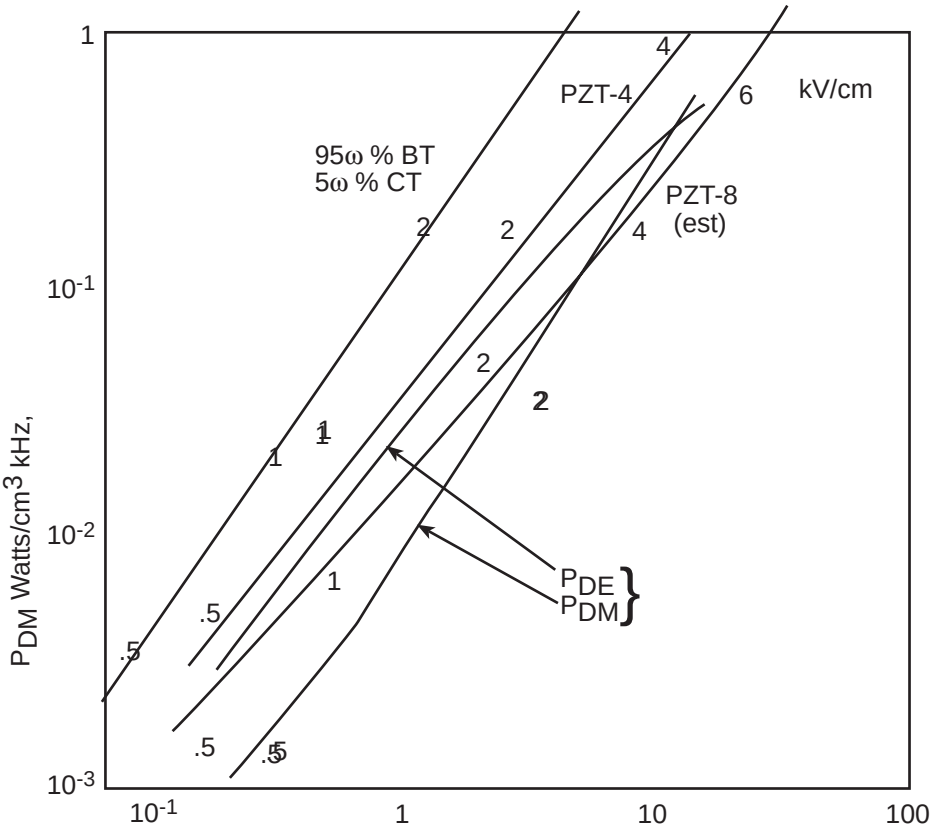

Fig. 10 Acoustic Power with Q_M=3, in Watts/cm^3 kHz

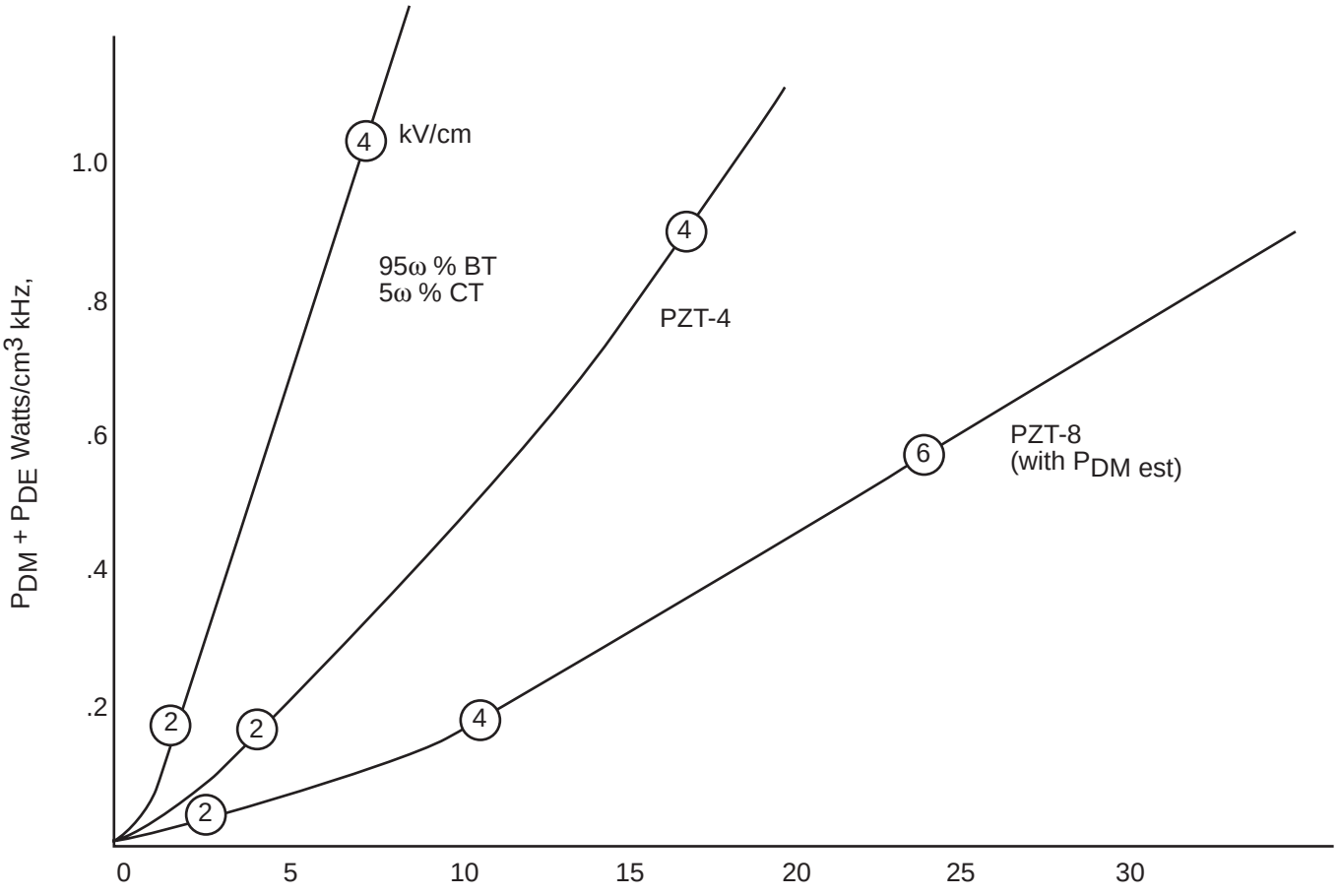

Fig. 11 Acoustic Power with Q_M=3, in Watts/cm^3 kHz

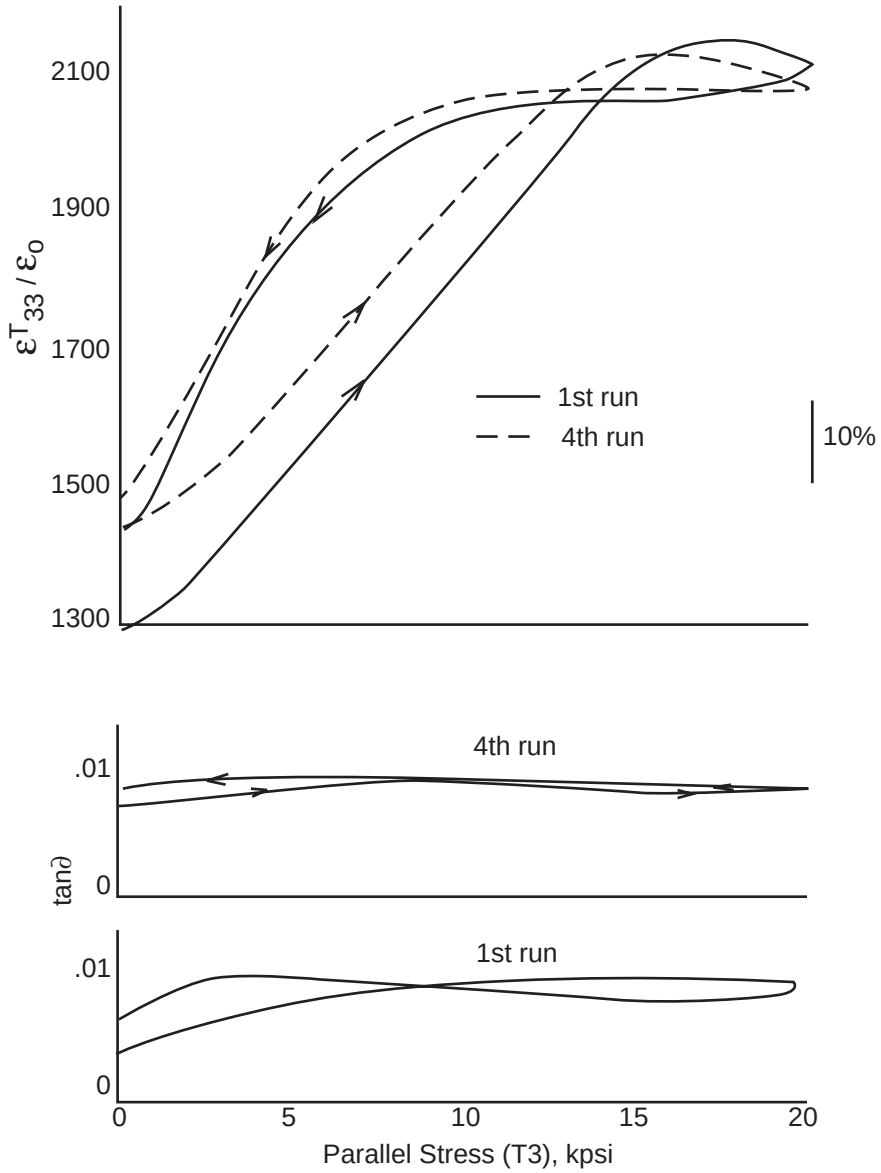

Fig. 12 $\varepsilon^T_{33} / \varepsilon_o$ vs parallel stress. PZT-4 (not stabilized)

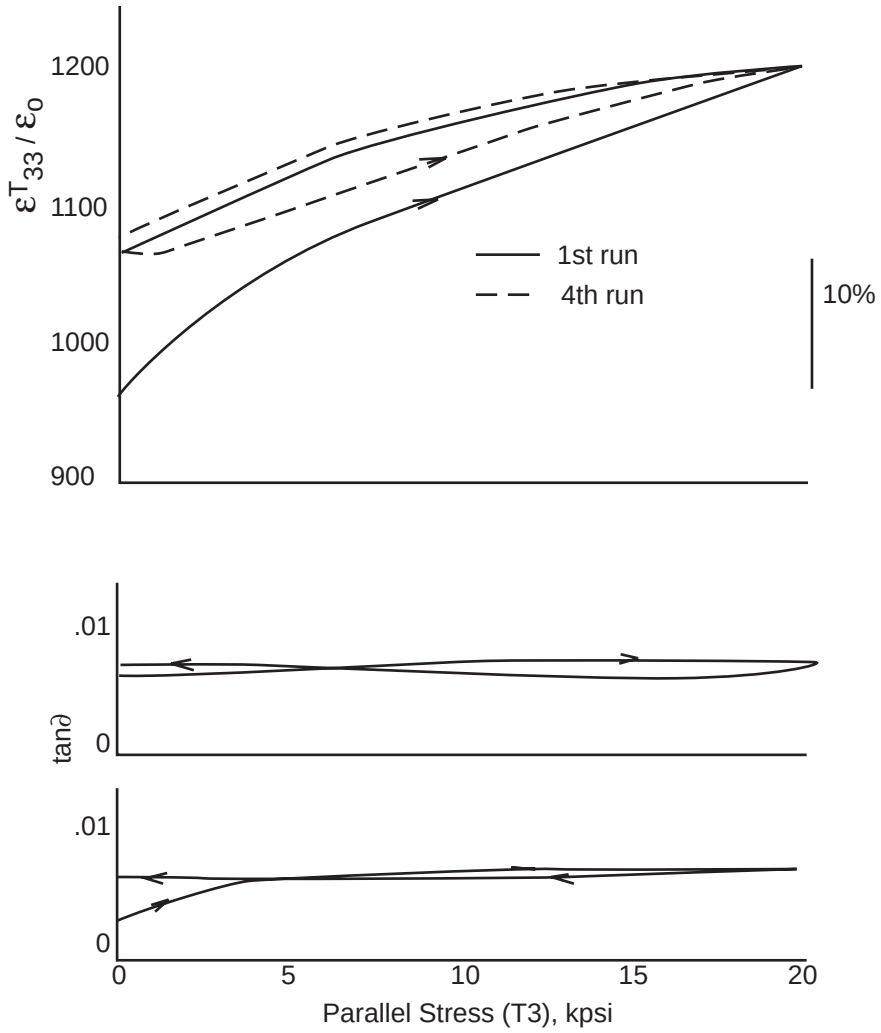

Fig. 13 $\varepsilon^T_{33} / \varepsilon_o$ vs parallel stress. PZT-4T (Tetragonal not stabilized)

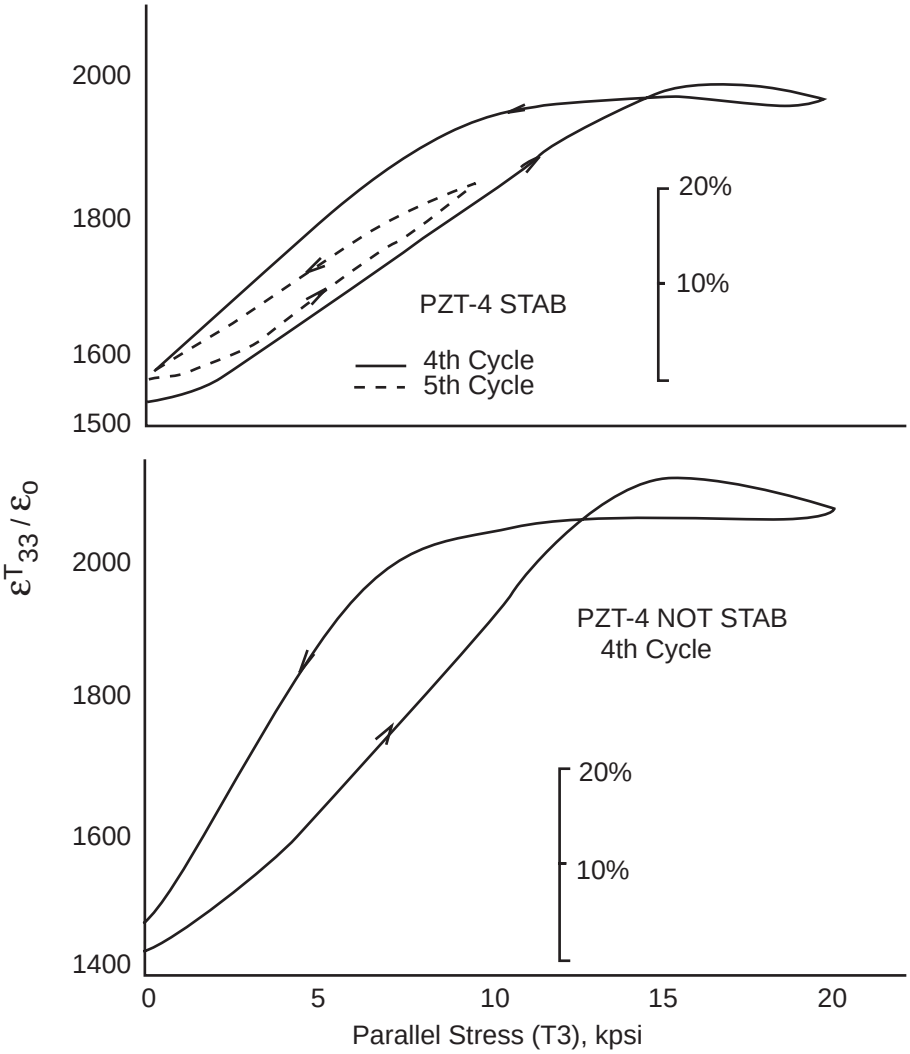

Fig. 14 $\varepsilon^T_{33} / \varepsilon_0$ vs parallel stress.

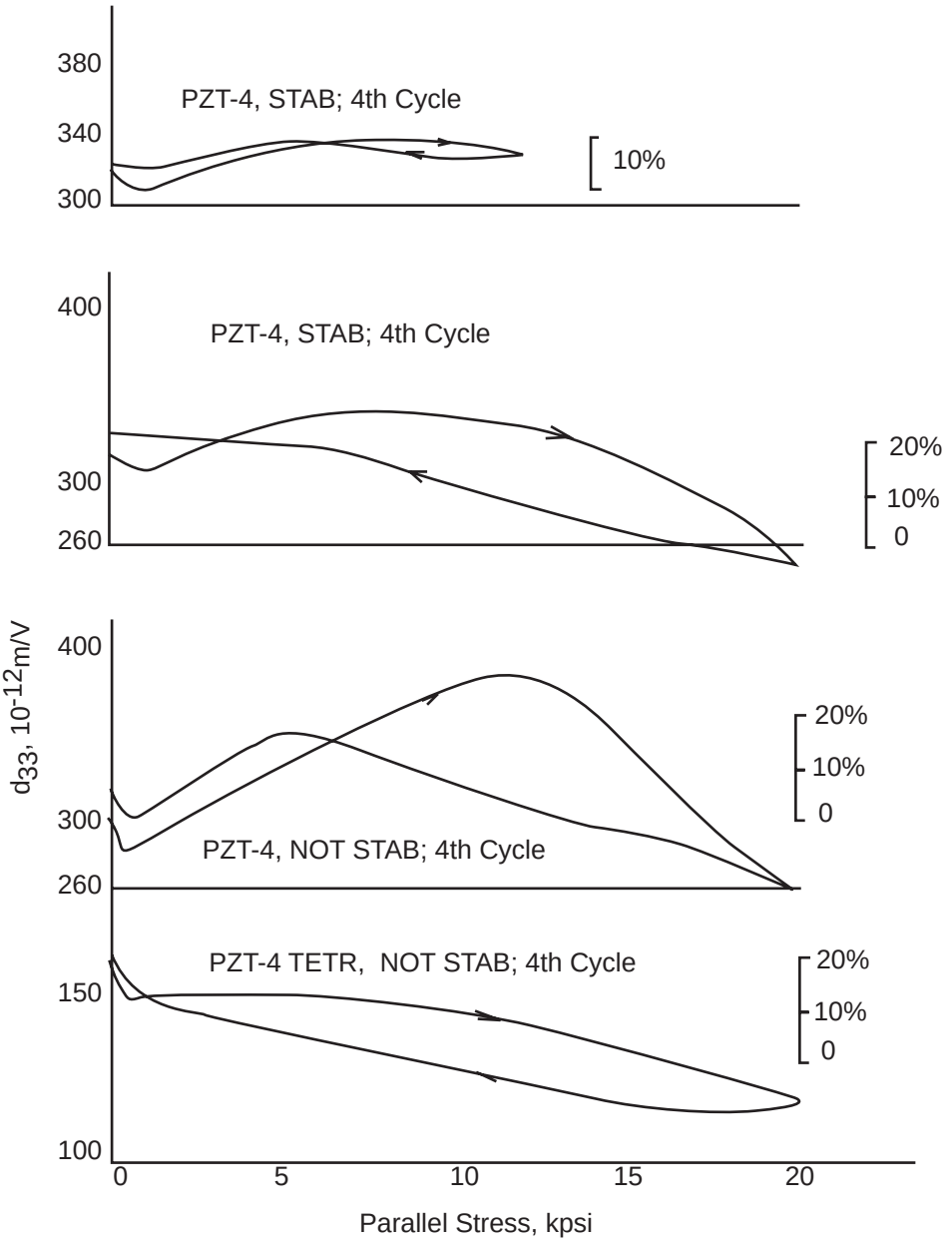

Fig. 15 d_{33} vs Parallel Stress

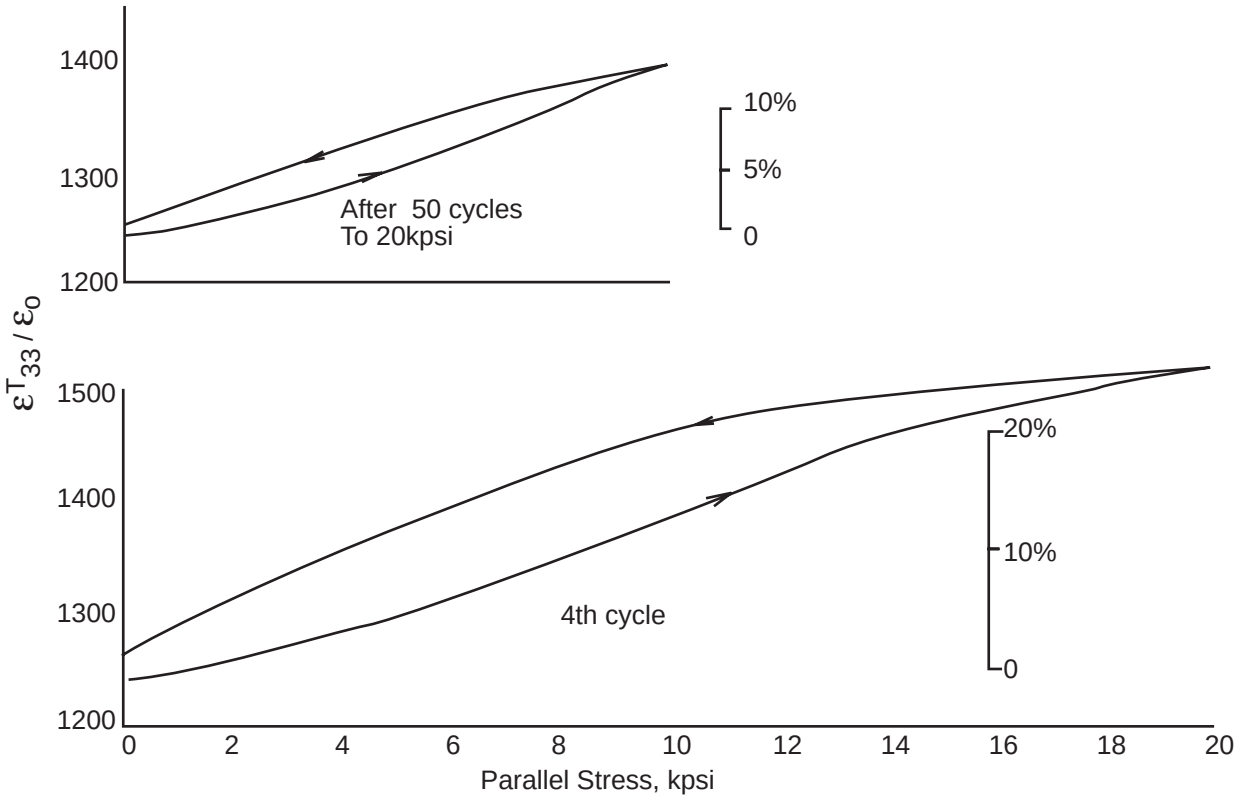

Fig. 16 $\varepsilon^T_{33} / \varepsilon_o$ vs parallel stress.

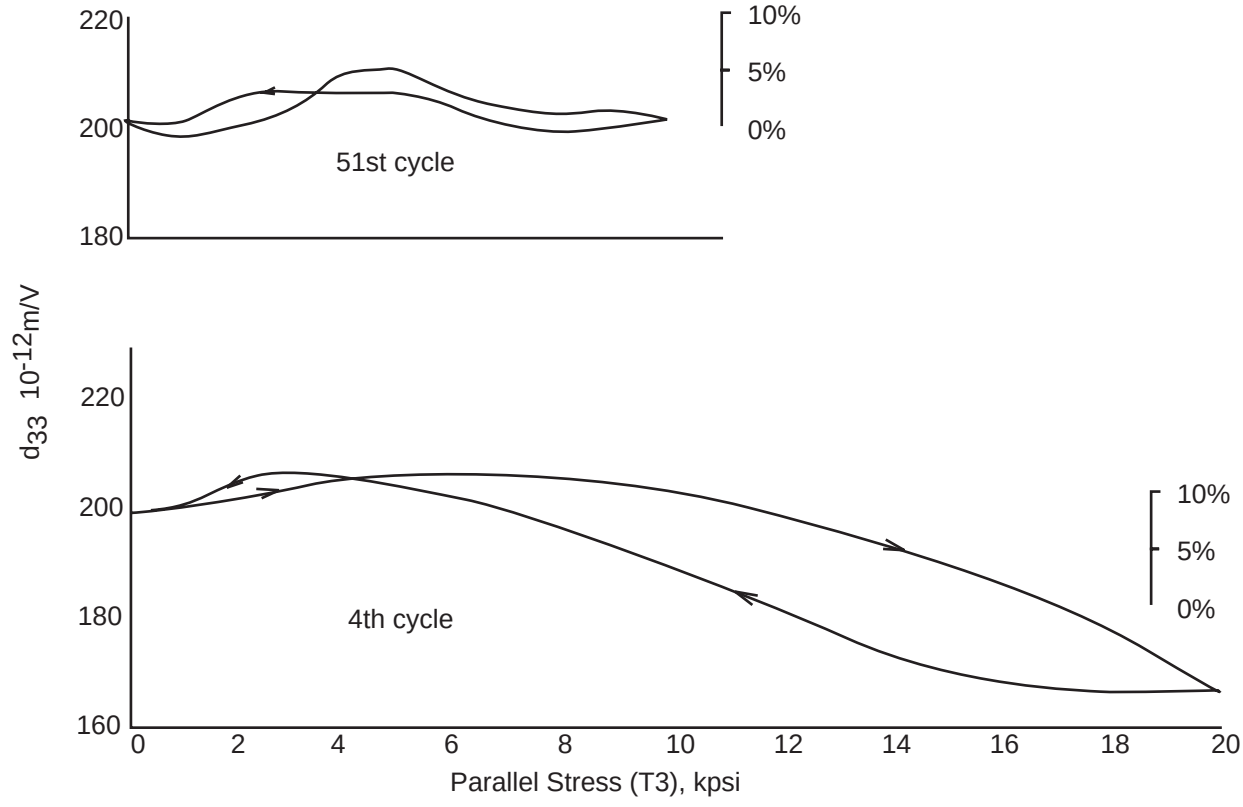

Fig. 17 d_{33} vs parallel stress.

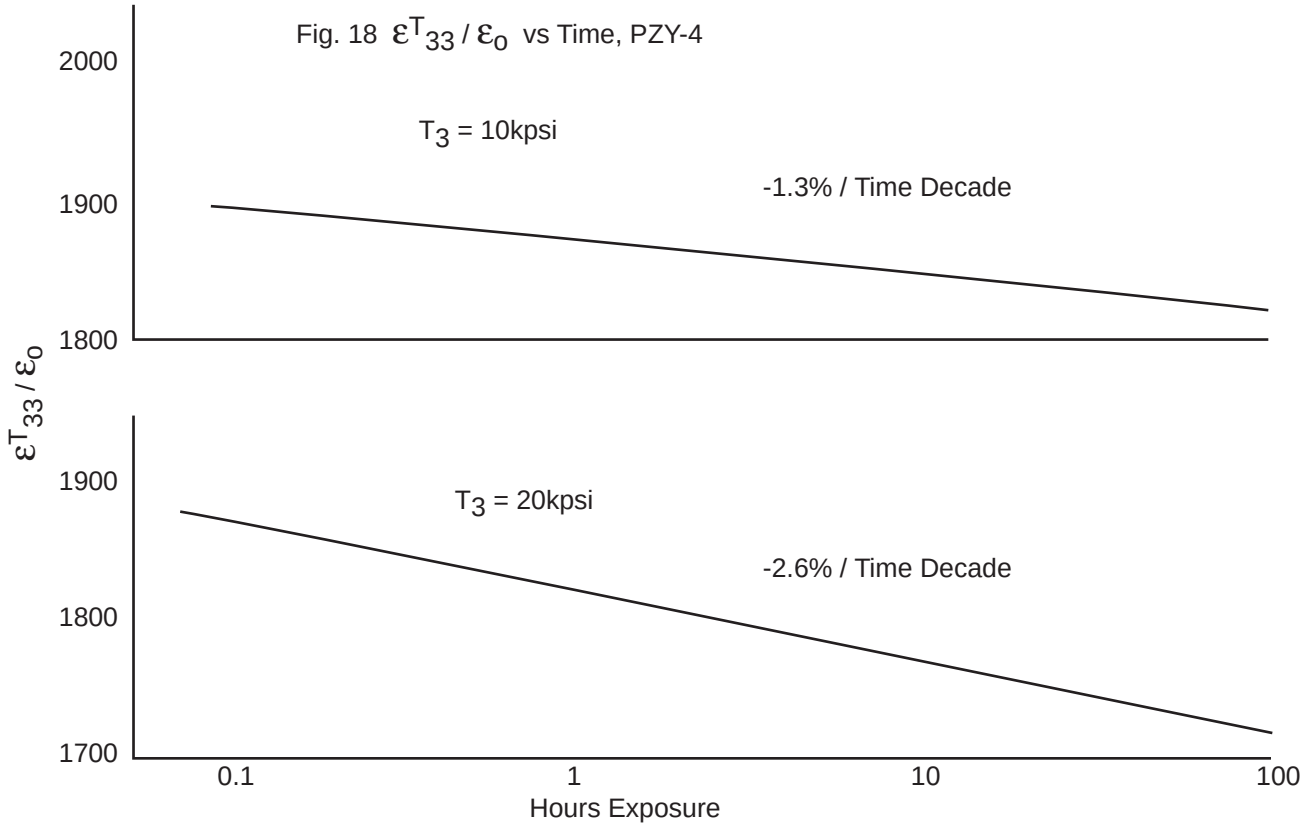

Fig.19 Aging of $d_{31}$and d_{32} with 10000psi compressive stress perpendicular (T_1) to the polar axis and aging of with 10000psi compressive stress parallel (T_3) to the polar axis for PZT-4. All measurements with stress maintained.

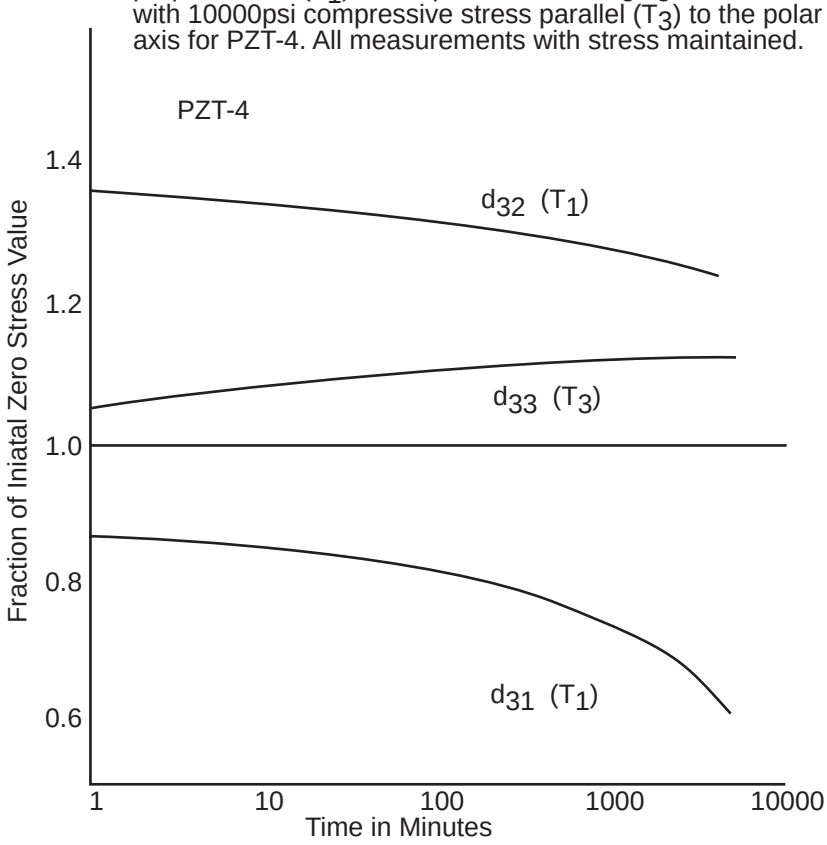

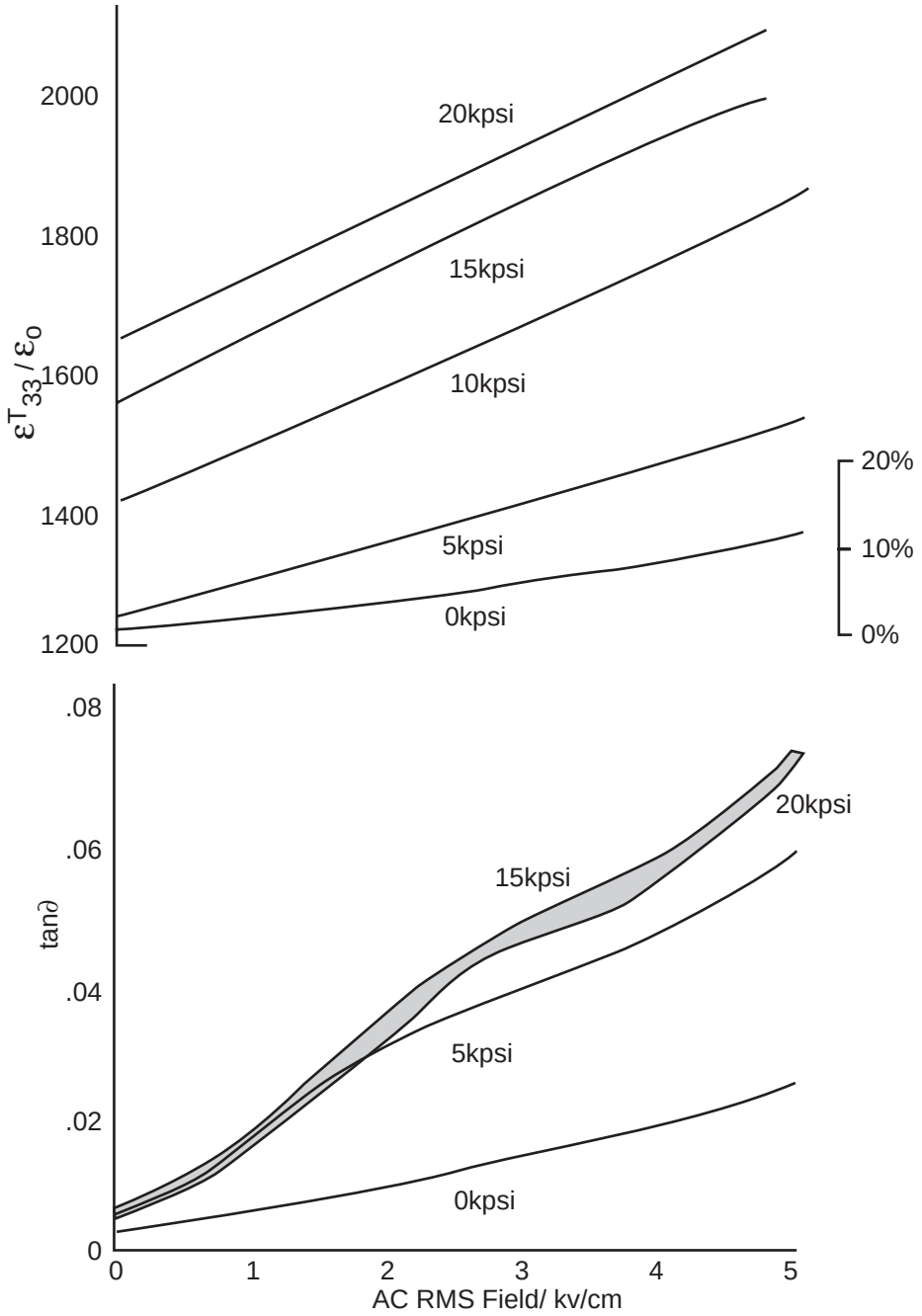

Fig. 20 $\varepsilon^T_{33} / \varepsilon_o$ and tan∂ vs AC field. Paramater; Longitudinal Stress (T_3) PZT-4)

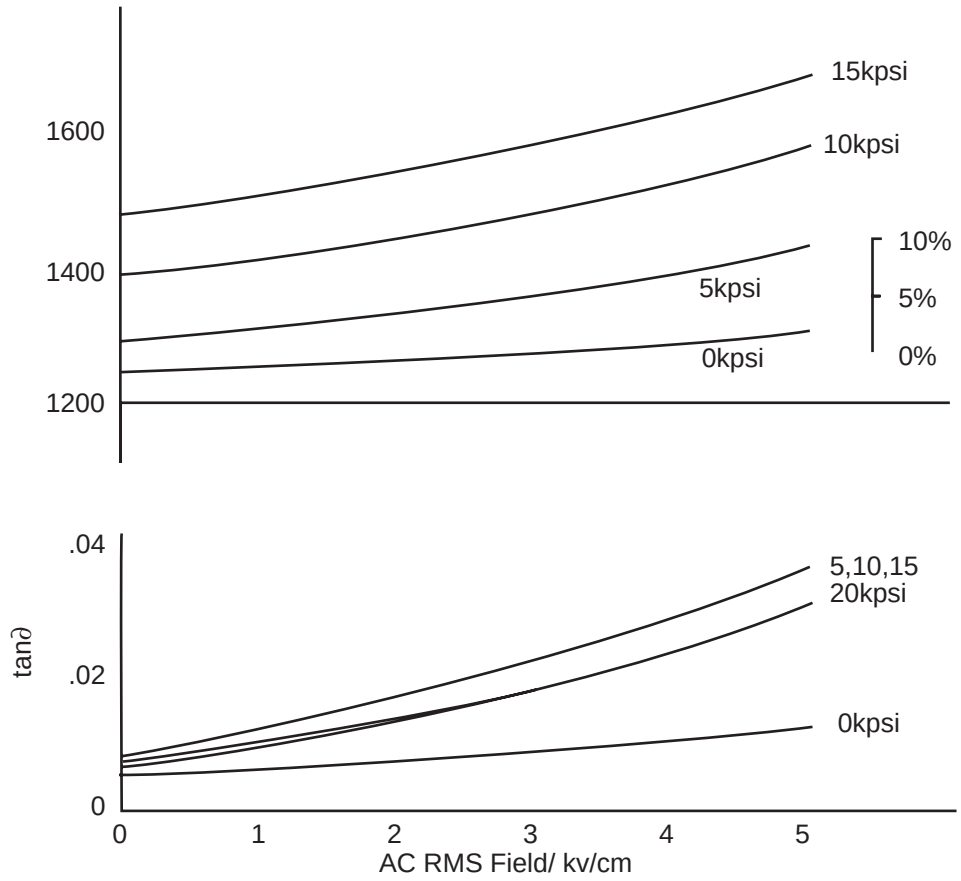

Fig. 21 $\varepsilon^{T}_{33} / \varepsilon_{o}$ and tanδ vs AC field. at various levels of parallel stress, PZT-8 (Not Stab)